Science Journal of Circuits, Systems and Signal Processing
2022; 10(2): 61-72
http://www.sciencepublishinggroup.com/j/cssp
doi: 10.11648/j.cssp.20211002.14
ISSN: 2326-9065 (Print); ISSN: 2326-9073 (Online)

Analysis of Design Parameters on Substation Earth Grid Safety Limits

Vuyani Michael Nicholas Dladla, Agha Francis Nnachi, Rembuluwani Philip Tshubwana

Department of Electrical Engineering, Tshwane University of Technology, Emalahleni, South Africa

Email address:

vuyo.dladla07@gmail.com (Vuyani Michael Nicholas Dladla), nnachiaf@tut.ac.za (Agha Francis Nnachi), tshubwanarp@tut.ac.za (Rembuluwani Philip Tshubwana)

To cite this article:

Vuyani Michael Nicholas Dladla, Agha Francis Nnachi, Rembuluwani Philip Tshubwana. Analysis of Design Parameters on Substation Earth Grid Safety Limits. *Science Journal of Circuits, Systems and Signal Processing*. Vol. 10, No. 2, 2022, pp. 61-72.
doi: 10.11648/j.cssp.20211002.14

Received: May 17, 2022; **Accepted**: June 10, 2022; **Published**: August 31, 2022

Abstract: In power systems, earthing is one of the most fundamental aspects that play a key role in ensuring the safety of personnel and equipment in a substation as well as reliable operation of the power system. Various elements within the earthing system scope play a vital role in ensuring compliance with relevant specifications, and these include design parameters such as soil resistivity, system fault level, conductor size, and the safety limits of touch voltage, step voltage, and the ground potential rise (GPR). In this paper, the influence of design parameters such as earth grid surface materials and asymmetrical fault currents on the design and performance of earthing systems are modeled, simulated, and analyzed. The Wenner four-pin method was used to conduct soil surveys and the collected data was used to design an earth grid according to the IEEE Std 80-2013 guidelines. The Electrical Transient Analyzer Program (ETAP) and MATLAB/Simulation engineering tools were used to model and analyze the design parameters. ETAP was used to assess the impact of different surface materials and MATLAB/Simulink was used to assess the influence of asymmetrical fault currents on the earth grid. From the analysis of the surface materials, it was observed that the crusher run granite is the most effective surface material for earth grids compared to the other surface materials studied. Furthermore, the impact of the surface material depth was studied using the crushed rocks, and results show that the depth of the surface material has an impact on the tolerable safety limits. Analyses were conducted in MATLAB/Simulink to assess the impact of asymmetrical faults (Line to Ground and Double Line to Ground) on touch voltage, step voltage, and ground potential rise. From the simulations, it was observed that the type of fault determines the magnitude of touch voltage, step voltage, and ground potential rise. From the analyses, it is concluded that the crusher run granite stones are the most effective surface material and should be used for earth grid designs, also, that the surface material should be buried as close to the surface as possible. Lastly, it is concluded that the type of system fault determines the magnitude of touch voltage, step voltage, and ground potential rise.

Keywords: Substation Earth Grid, Touch Voltage, Step Voltage, Ground Potential Rise, ETAP, MATLAB/Simulink

1. Introduction

As part of a substation design scope, the earthing system is an integral part that is always considered in the feasibility phase. The main objective of earthing systems is to ensure the safety and protection of personnel who get exposed to conductive structures and energized electrical equipment, it achieves this by directing the fault currents to earth through a low resistive path made up of earth grid elements such as horizontally buried conductors, vertically driven earth electrodes, and earth risers.

This paper presents an extension of a paper originally presented at the *2019 IEEE 62nd International Midwest Symposium on Circuits and Systems (MWSCAS)* [1], where an analytical method for determining the resistance of an earth grid was developed. To evaluate the effectiveness of this method under transient conditions, an earth grid was modeled in MATLAB/Simulink and applied to an 88/22kV, 20MVA substation, which was then simulated to assess the earth grid performance [1]. The safety limits of touch voltage, step voltage, and ground potential rise were assessed under symmetrical fault conditions and the results were presented.

The earth grid directs transient currents into the ground through a low resistive path [2], this helps to restrict elevated voltages on the safety limits parameters of step voltage, touch voltage, and the ground potential rise [3-5].

For an optimum earth grid design that caters to safety, reliability, and financial aspects of the design and implementation, various elements such as soil resistivity, conductors, and system fault level are thoroughly analyzed [6]. Studies by V. P. Androvitsaneas et al. and N. Permal et al. [7, 8] found that soil resistivity and system fault level have a great impact on the performance of the earth grids as they directly affect the GPR, and according to IEEE Std 80-2013 [9], GPR is a parameter used and compared with touch voltage and step voltage to assess the tolerable limits of the earth grid.

The influence of various design parameters such as asymmetrical fault currents, system fault level, soil resistivity, and earth grid surface materials on the performance of earthing systems is modeled, simulated, and analyzed in MATLAB/Simulink and the Electrical Transient Analyzer Program (ETAP) software. The earth grid is designed based on the IEEE Std 80-2013 guidelines and requirements.

2. Earthing System Design Considerations

In the design phase of an earth grid, various elements should be considered concerning the design and performance of an earth grid such as the vertically driven earth electrodes, the buried earth conductors, the substation area soil resistivity, and the supply system fault level [3].

2.1. Soil Resistivity

Soil resistivity is defined by IEEE Std 81-2012 [10] as the measure of current flowing through the soil constantly resisted by a certain volume of soil. In the design process of the earthing grids, the soil resistivity parameter comes into play when computing the safety limits of Touch Voltage (TV) and Step Voltage (SV), and the maximum grid resistance. Studies conducted by IEEE Std 80-2013, L. L. Win et al., and N. H Amandi et al. [9, 11, 12] show that soil resistivity is influenced by various environmental factors and soil properties such as the type of soil, moisture, and salt content in the soil, the temperature of the soil, and the conductive nature of the soil studied. Figure 1 shows the impact of different soil properties on soil resistivity [2, 9].

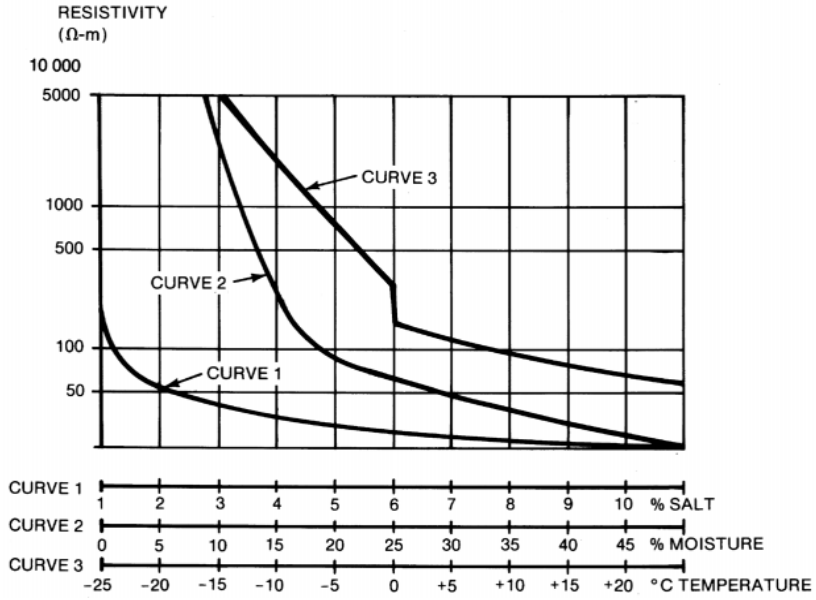

Figure 1. *Effects of different soil properties on soil resistivity [9].*

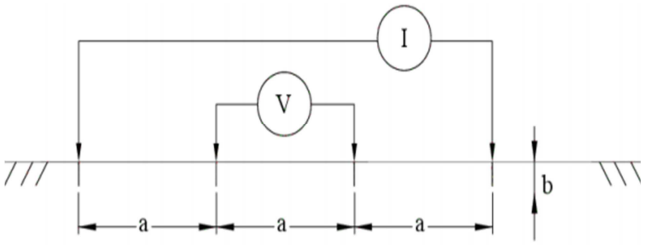

Figure 2. *Wenner four-pin method configuration [14].*

To determine the soil resistivity of various soil types for design and analysis purposes, the Wenner four-pin method is a widely used method to conduct soil resistivity measurements. The soil resistivity measurements are conducted by driving four earth electrodes into the ground which must be arranged in a straight line and equally spaced between each other. The two outer electrodes are used to inject current from the measuring equipment into the ground, the two inner electrodes then measure the resultant voltage drop caused by the soil resistivity [1, 13, 14]. Figure 2 shows the Wenner four-pin method configuration.

The Wenner four-pin method can be expressed as follows to obtain the measured soil resistivity:

$$\rho_a = \frac{4\pi aR}{1+\frac{2a}{\sqrt{a^2+b^2}}-\frac{2a}{\sqrt{4a^2+4b^2}}} \quad (1)$$

Where:

ρ_a is the apparent soil resistivity for spacing a;

R is the ratio of voltage across the inner probes to the outer probes injected current;

a is the distance between the equally spaced electrodes;

c is the depth of the electrodes.

2.2. System Fault Level

In a power system, transformers are used to step up or step-down voltages depending on the application it is required for. Transformers come in different sizes and properties, and one of the most important properties of transformers is their apparent power and impedance. Using the rated transformer's apparent power and impedance, one can determine the fault level that can be generated by the transformer [3, 15].

Various factors affect the system fault level, and these factors should always be carefully considered when conducting short-circuit studies for power system design [16]. Technically, the power system's faults occur and operate differently, these unique properties are used to classify them when system studies are conducted as shown below [3, 17].

1) Prospective fault current, Steady-state fault current;
2) Peak fault current;
3) Symmetrical fault current, and
4) Asymmetrical fault current.

2.3. Earth Conductors and Electrodes

One of the essential elements required in an earth grid and that are carefully selected to achieve low resistance are earth electrodes [3, 18]. Depending on their application, earth electrodes come in various types which include copper, aluminium, stainless steel, and iron cast [9].

In most cases, several electrodes are required to achieve low resistance, but in some cases where the soil has high water content, a single earth electrode may be required to achieve low resistance [3, 19].

Depending on the earth electrode design requirements, various parameters are considered such as the size of the earth electrode, the material used, the numbers of electrodes, and the depth at which it is installed [3, 11]. Furthermore, since soil resistivity directly affects the earth electrode's resistance [11], it is important to consider and analyse this parameter during the design phase. The earth electrode's resistance can be computed using (2).

$$R_{each} = \frac{\rho}{2\pi L}\left[\log\left(\frac{8L}{d}\right) - 1\right] \quad (2)$$

Where:

ρ is the soil resistivity;

L is the length of the electrode;

d is the cross-sectional diameter of the electrode.

3. Substation Earth Grid Design Requirements and Qualifications

The substation earth grid plays a vital role in ensuring the safety and protection of people and equipment as well as maintaining the stability and reliability of the power system [3]. According to the earth grid design guidelines as set out by IEEE Std 80-2013 [9], various design elements such as the soil resistivity, earth grid fault current, touch voltage, step voltage, and ground potential rise are thoroughly assessed to ensure an optimum earth grid design is achieved [2].

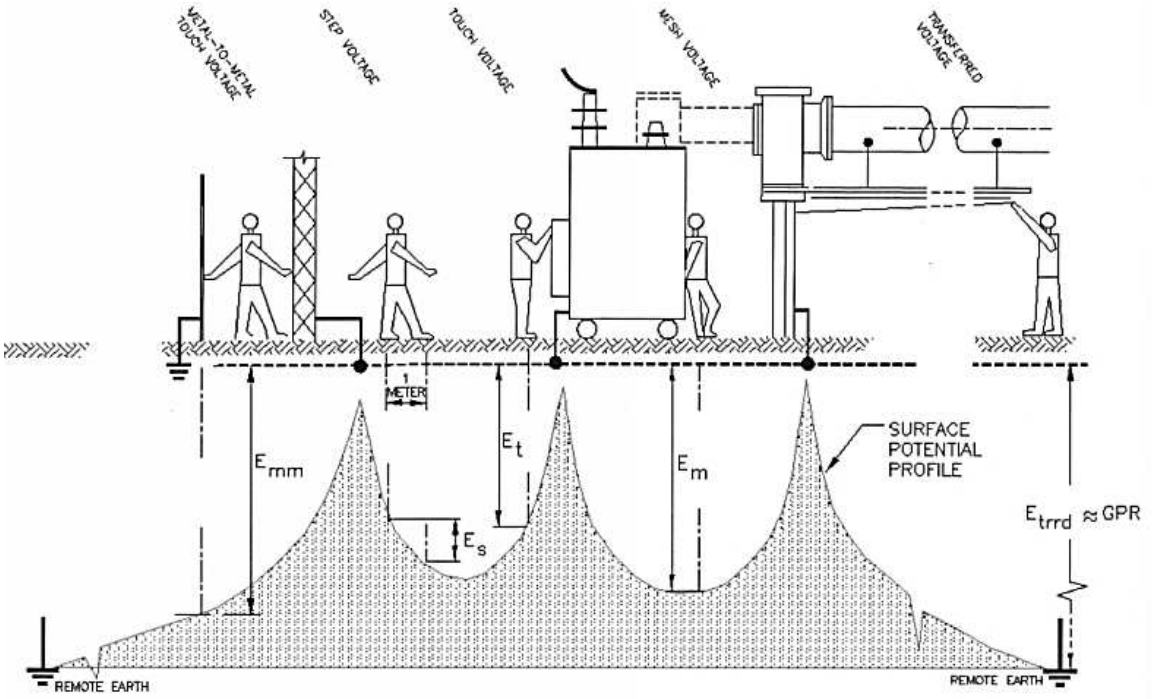

Figure 3. *Various shock situations in a substation [9].*

3.1. Safety Limits

The major parameters of an earthing system used to verify the compliance of an earth grid are the safety limits of touch voltage, step voltage, and the ground potential rise. The ground potential rise is defined as the maximum source potential that can be generated in an earth grid with respect to a common grounding terminal in the grid, and touch voltage is defined as the potential difference between the surface potential and the ground potential rise [9, 20]. Step voltage is further defined as the surface potential across the feet of a person without that person making any contact with an object that is energized and connected to ground reference [9, 20]. Figure 3 shows the various shock situations in a substation.

3.2. Design Criteria

The computation of the IEEE Std 80-2013 guidelines consists of various steps (step 1 to step 12) as shown in Figure 4 on which certain design and performance conditions are tested and must be met.

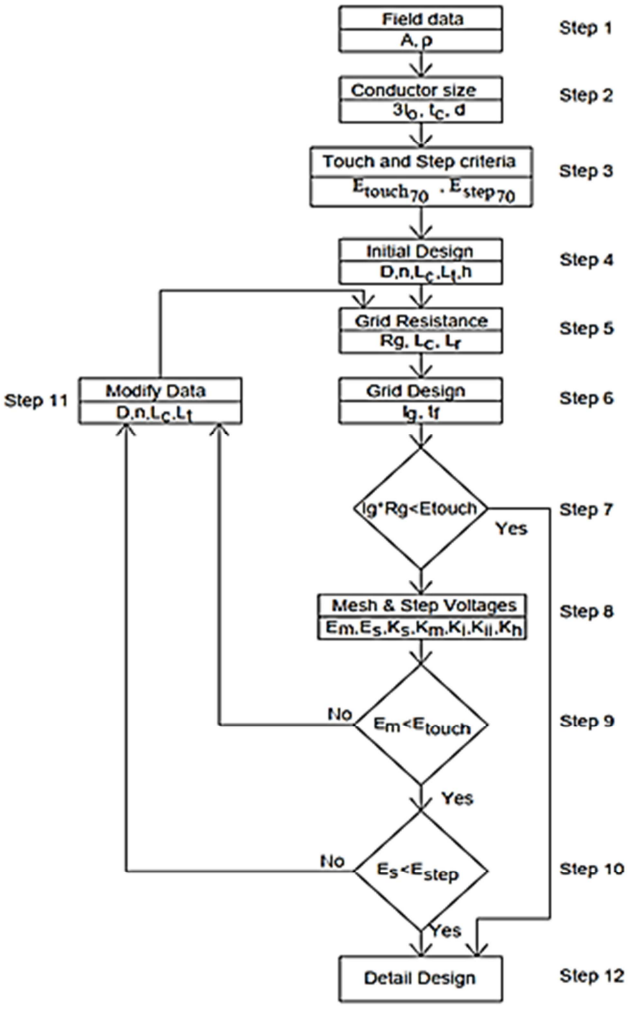

Figure 4. *IEEE Std-80 earthing grid design flowchart [9].*

Under ideal design conditions, the design requirements are satisfied at step 7, but in cases where the Ground Potential Rise is greater than the Touch Voltage, further calculations are required to assess the Mesh Voltage and the Step Voltage between the points above the outer corners of the grid as shown in step 9 and step 10 of the IEEE Std-80-2013 guidelines [9] and in the study conducted by V. M. N. Dladla et al. [2]. The results of these calculations are then verified for compliance against Touch and Step Voltage using the IEEE Std 80-2013 design requirements.

4. Substation Earth Grid Design, Modelling, and Analysis

4.1. Earth Grid Design

For this study, the IEEE Std 80-2013 method was used, adhering to the design flow chart shown in Figure 4. For the calculations, input data was gathered for a representative substation modeled by B. Z. Nongena [1], where the Wenner four-pin method was used to obtain the respective soil resistivity of the substation area. From the populated input data, earth grid elements such as the cross-sectional area of the earth electrodes and buried conductors were determined using the earth grid design parameters namely, the system fault level generated by the supply transformer, the estimated worst-case scenario fault duration, and the material constant for annealed soft-drawn copper provided in IEEE Std 80-2013 [2]. Using the transformer parameters provided on the nameplate, the system fault current was determined using (3).

$$I_{sc} = \frac{S}{\sqrt{3} \times V \times z} \tag{3}$$

where:

S is the transformer's apparent power;

V is the system voltage;

z is the source transformer impedance in p.u.

By implementing the IEEE Std 80-2013 guidelines for earth grid design as shown in Figure 4, the substation earth grid safety limits of Touch Voltage, Step Voltage, and the Ground Potential Rise using (4), (5), and (8), respectively were calculated [2]. Using the surface material resistivity of crushed rocks on an estimated shock duration of 0.15 seconds the safety limits of Touch Voltage and Step Voltage were determined to be 2214 V and 7639 V respectively.

$$E_{step70} = (1000 + 6C_s \cdot \rho_s)\frac{0.157}{\sqrt{t_s}} \tag{4}$$

$$E_{touch70} = (1000 + 1.5C_s \cdot \rho_s)\frac{0.157}{\sqrt{t_s}} \tag{5}$$

where:

C_s is the surface layer derating factor;

ρ_s is the resistivity of the surface material;

t_s is the duration of shock current.

As demonstrated in the guidelines provided by IEEE [9] and calculations conducted by V. M. N. Dladla et al. [20], the earth grid resistance (6) can be obtained using the soil

resistivity obtained using the Wenner four-pin method (1), the depth of the earth conductors, and the sum of the earth grid conductors and earth electrodes length. The calculated earth grid resistance using (6) was found to be R_g = 0.665 Ω.

$$R_g = \rho\left[\frac{1}{L_T} + \frac{1}{\sqrt{20A}}\left(1 + \frac{1}{1+h\sqrt{20/A}}\right)\right] \quad (6)$$

where:

ρ is the soil resistivity;

A is the earthing mat area;

h is the depth of the ground grid conductor;

L_T is the total length of grounding system conductors and ground rods.

Based on the calculated system fault current in (3), the maximum grid current (7) was found to be I_G = 7.22kA.

$$I_G = 3I_0 D_f S_f \quad (7)$$

where:

$3I_0$ is the system fault current;

D_f is the decrement factor;

S_f is the current division factor.

To determine the GPR, the grid resistance (6), and the maximum grid current (7) parameters were obtained, using these parameters on (8), a GPR value of 4804V was obtained.

$$GPR = I_G R_g \quad (8)$$

Where:

I_G is the maximum grid current;

Rg is the earth grid resistance.

Since the design criteria are not met by step 7, further calculations should be conducted as computed in the study carried out by V. M. N. Dladla et al. [2] to determine the mesh voltage (step 9) and Step Voltage (step 10) of the design flowchart as shown in Figure 4.

The results of the overall calculation are summarized and tabulated in Table 1:

Table 1. *Calculated Earth Grid Design Parameters.*

No.	Parameter Description	Calculated value
1	Conductor size, A_c	35 mm^2
2	Tolerable Step Voltage, E_{step70}	7639 V
3	Tolerable Touch Voltage, $E_{touch70}$	2214 V
4	Ground Resistance, R_g	0.67 Ω
5	Maximum Grid Fault Current, I_g	7.22 kA
6	Ground Potential Rise, *GPR*	4804 V
7	System Mesh Voltage, E_m	527.3 V
8	Step Voltage between outer corners of the grid, E_s	287.75

4.2. Modeling and Analysis

From the calculations and design qualifications estimated in Section III, the earth grid was modeled for simulations in ETAP, a 70m x 70m earth grid consisting of 11 x 35 mm^2 earth conductors arranged in the x-direction and 11 x 35 mm^2 in the y-direction, equally spaced between each other at 7m apart covering an area of 4900m^2. The earth also consists of 20 earth electrodes installed on the perimeter of the earth grid at 3m depth. Figure 5 shows an earth grid modeled in ETAP.

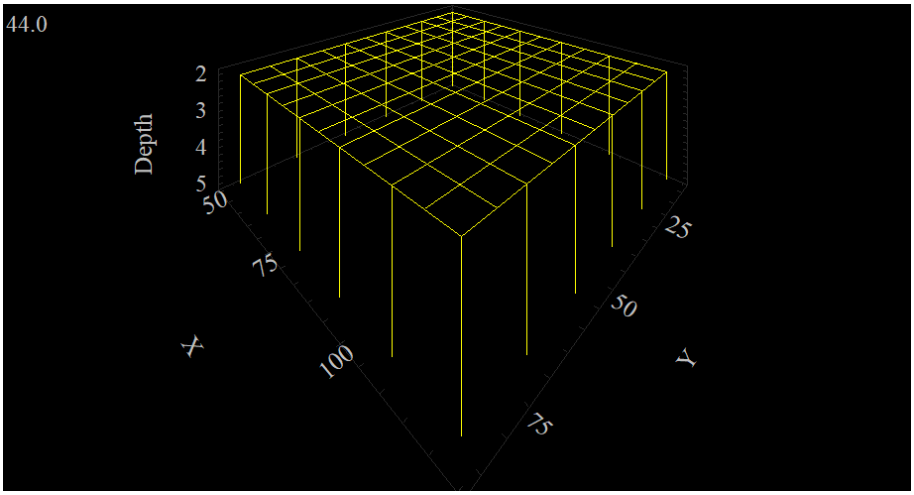

Figure 5. *A 70 m x 70 m square-shaped earth grid with earth electrodes on the perimeter of the grid.*

The results were further presented graphically using contour plots to show the different voltage profiles that are present along the grid. The simulation results are shown in Figures 6, 7, and 8 illustrating the touch voltage, step

voltage, and ground potential rise, respectively. Figure 6 shows the earthing grid step voltage profile, and it shows that the voltage levels throughout the entire grid are within the safe, low voltage threshold ranging from 0 V to 650 V, which is well below the tolerable step voltage limit of 7638.7 V.

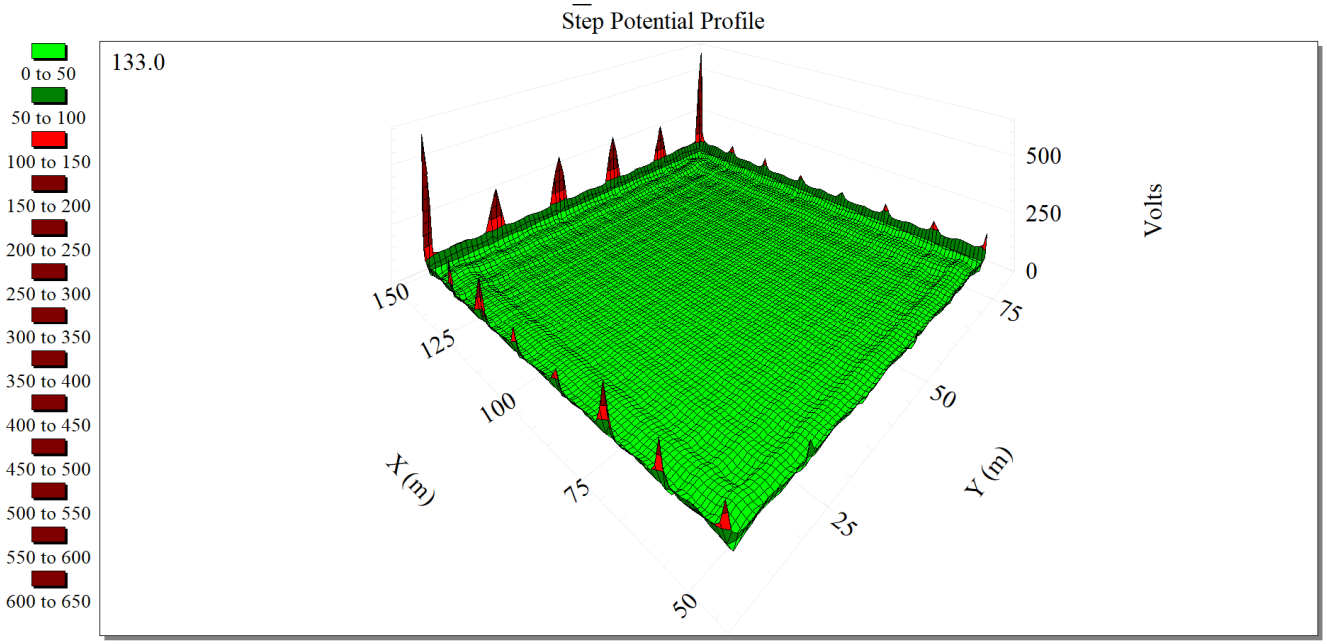

Figure 6. *Grounding grid step voltage profile.*

Figure 7 shows the earth grid's touch voltage profile and from the simulation results, it is observed that the voltage levels vary throughout the grid. In the central part of the grid, the touch voltage limits are within the 0 V to 150 V range and spread to 150 V to 200 V. The voltage further varies to higher values on the perimeter of the grid where it reaches voltages high as 550V. Even though the voltage varies throughout the grid from 0 V up to 550V, it is still well within the tolerable touch voltage limits of 2213.7 V.

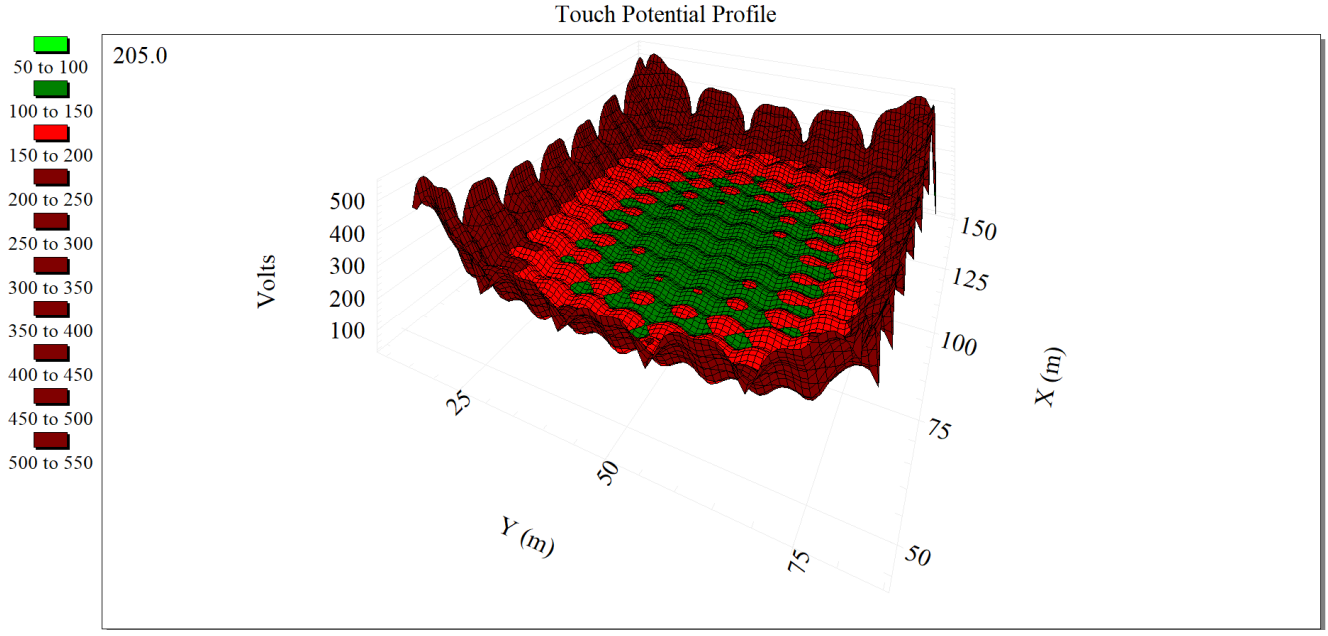

Figure 7. *Grounding grid touch voltage profile.*

In Figure 8, the simulated earth grid's absolute potential profile is illustrated. From the voltage readings, it can be observed that the earth grid voltage is 4802.2V, unlike the step voltage and the touch voltage, the simulation settings for the ground potential rise do not show the overvoltage limits, as a result, the absolute potential profile only shows the green color.

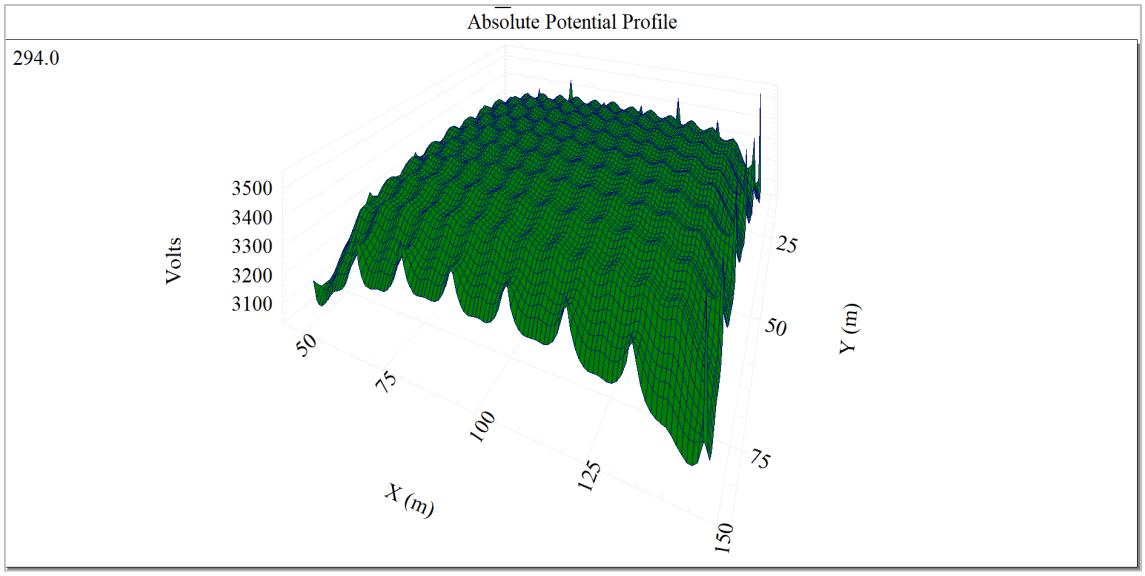

Figure 8. *Grounding grid ground potential rise profile.*

4.3. The Impact of Surface Material

Further simulations were conducted to assess the impact and influence of the surface material used in switchyards, there are different methods used to try and limit the step and touch potential low as possible in the substation and one of the most used methods is spreading surface materials such as crushed rocks around the substation [21]. Different surface materials were simulated with their unique resistivity to assess their impact on the touch and step voltage.

Table 2 shows the impact each material has on the safety limits of touch and step voltage. From the results, it is observed that the crusher run granite, which has the lowest material resistivity, has the least impact on the tolerable touch and step voltage, while gravel with the highest material resistivity has the greatest impact on the tolerable touch and step voltage.

Table 2. *The impact of surface material types on touch and step voltage.*

Surface material type	Material Resistivity (Ωm)	Touch Voltage (V)		Step Voltage (V)	
		Calculated	Tolerable	Calculated	Tolerable
Crusher run Granite	1318.7	790.5	977.2	218.1	2692.8
Clean Limestone	2500	790.5	1472.6	218.1	4674.4
Crushed rock	4267.2	790.5	2213.7	218.1	7638.7
#57 clean granite	8106.8	790.5	3823.8	218.1	14079.2
Gravel	8534.4	790.5	4003.1	218.1	14796.5

With the surface materials known to have different impacts on the safety limits, it also very important to assess the depth at which these materials are most effective and practicably feasible to solidly lay down without being washed off by heavy rains or movement of heavy machinery. For simulation purposes, the surface material depth of *Crushed rocks* was assessed at different depths and the results are tabulated in Table 3. The results show that the depth at which the surface material is laid is directly proportional to the tolerable touch and step voltage.

Table 3. *The impact of surface material depth on touch and step voltage.*

Surface material depth (cm)	Touch Voltage (V)		Step Voltage (V)	
	Calculated	Tolerable	Calculated	Tolerable
50	790.5	1799.8	218.1	5983.1
100	790.5	2213.7	218.1	7638.7
150	790.5	2415.3	218.1	8445.2
200	790.5	2534.7	218.1	8922.6

4.4. The Impact of Asymmetrical Faults

From the simulation conducted by B. Z. Nongena [1], the safety limits of touch voltage, step voltage, and ground potential rise were modeled and analyzed under symmetrical fault conditions. For further analysis, the earth grid was modeled in MATLAB/Simulink, and asymmetrical fault currents were injected into the earth grid for analysis and to evaluate the

impact of these faults on the safety limits. The earth grid model in MATLAB/Simulink is shown in Figure 9 with 11 conductors in the x-direction and 11 conductors in the y-direction and having 20 earth electrodes installed on the perimeter of the grid.

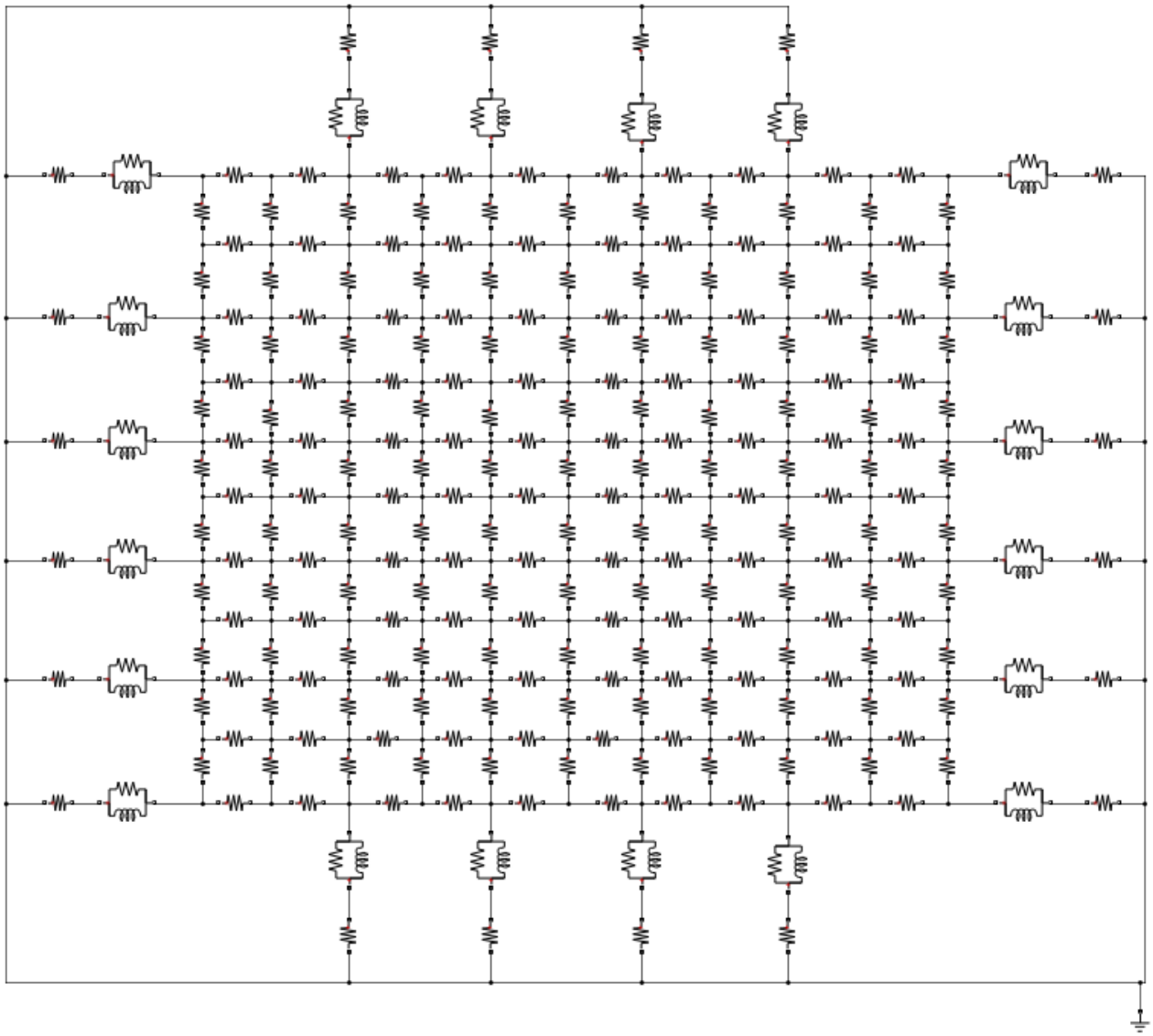

Figure 9. *A square-shaped earthing grid with earth electrodes on the perimeter of the grid.*

To better assess and evaluate the impact of asymmetrical fault currents on the power system, an earthing grid was modeled, and the asymmetrical faults of the Line-Ground fault and Line-Line-Ground fault were simulated and analyzed. The results of the simulations including voltage and current waveforms profiles of the power system, and waveforms of touch voltage, step voltage, and ground potential rise are shown in Figures 10 to Figure 17.

4.4.1. The Line to Ground Fault

A study on fault types conducted by V. M. N. Dladla et al. [3] suggests the Line-Ground fault occurs when one of conducting phases gets in contact with or is short-circuited with the ground, the study further states that the voltage of the phase in contact with the ground drops to zero while the magnitude of the unaffected phases doubles, in support of this study, it can also be observed in Figure 10 on the secondary voltage waveform that when the fault is injected into the power system between 0.08 and 0.15 seconds, the voltage magnitude of faulted yellow phase drops close to zero while the magnitude of the red and blue phases almost doubles in size.

In the same study, V. M. N. Dladla et al. [3] further suggest that the current magnitude of the affected phase that contacts the ground rises significantly. These findings can also be observed in Figure 10 of the power system secondary current waveform, when the fault is injected into the system between 0.08 and 0.15 seconds, the current magnitude of the faulted yellow phase increases significantly.

In Figure 10, the secondary voltage and current waveforms under the Line-Ground fault are shown, in Figures 11 to 13, the impact of the Line-Ground fault current on touch voltage, step voltage, and ground potential rise, are shown respectively.

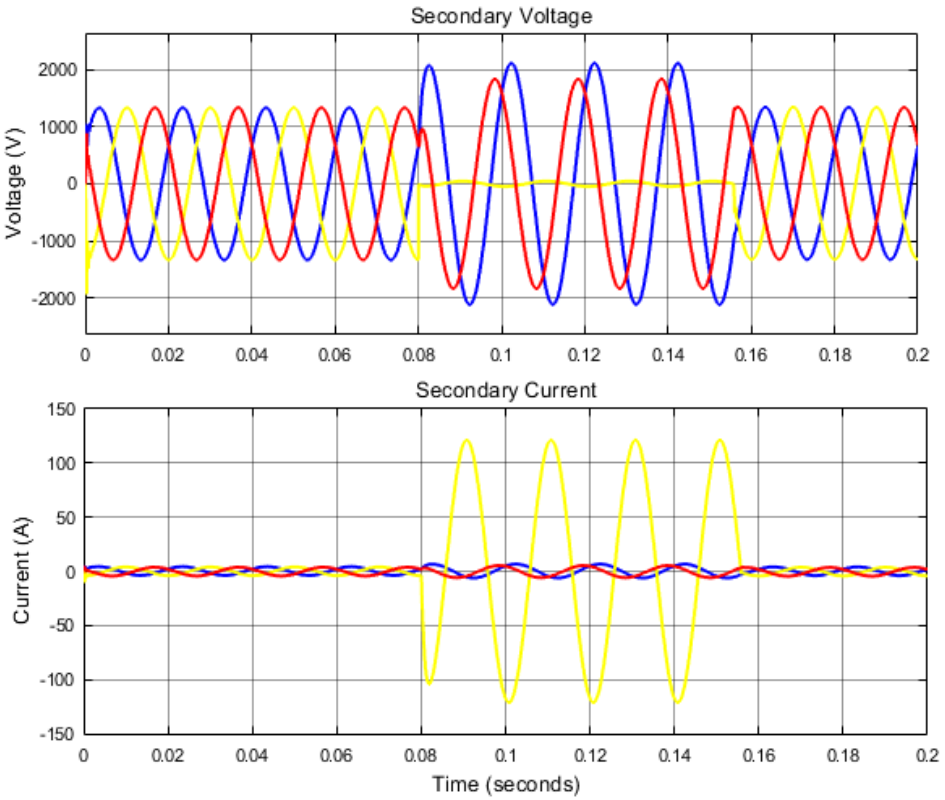

Figure 10. *Supply Voltage and Current under Line-Ground Fault.*

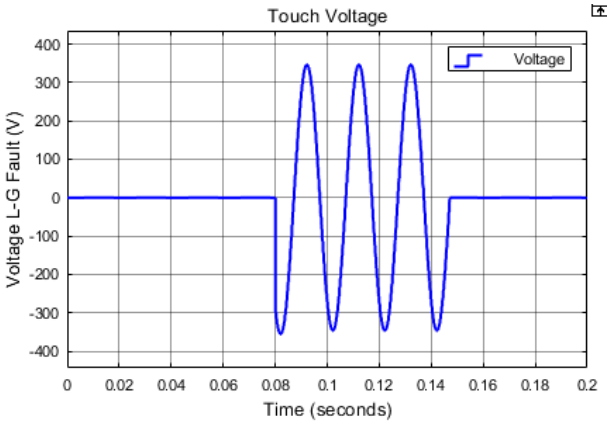

Figure 11. *Touch Voltage under Line- Ground Fault.*

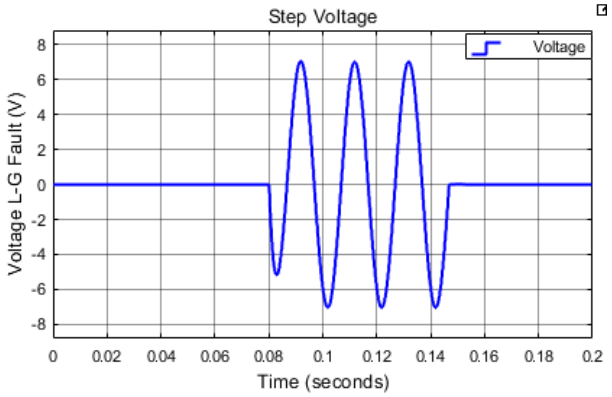

Figure 12. *Step Voltage under Line- Ground Fault.*

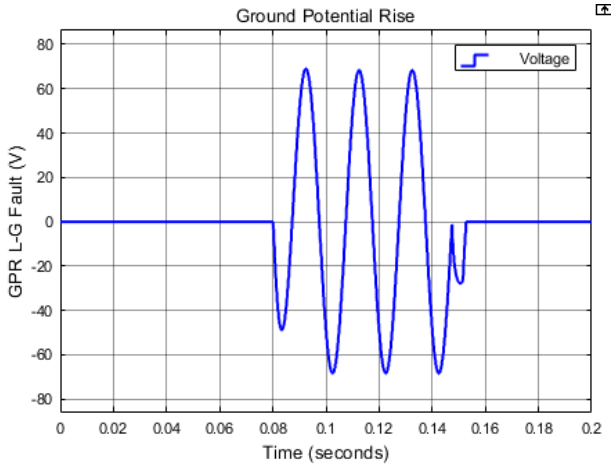

Figure 13. *Ground Potential Rise under Line- Ground Fault.*

4.4.2. The Line to Line to Ground Fault

Similar to the Line-Ground fault, the Line-Line-Ground fault occurs when two conducting phases of a power system get in contact with or are short-circuited with the ground, the voltage magnitude of the affected phases drops to zero while the magnitude of the unaffected phase doubles as observed by V. M. N. Dladla et al. [3]. In support of this study, it is observed in Figure 14 on the secondary voltage waveform that when the fault is injected into the power system between 0.08 and 0.15 seconds, the voltage magnitude of faulted yellow and blue phases drops close to zero while the magnitude of the unaffected red phase almost doubles in size.

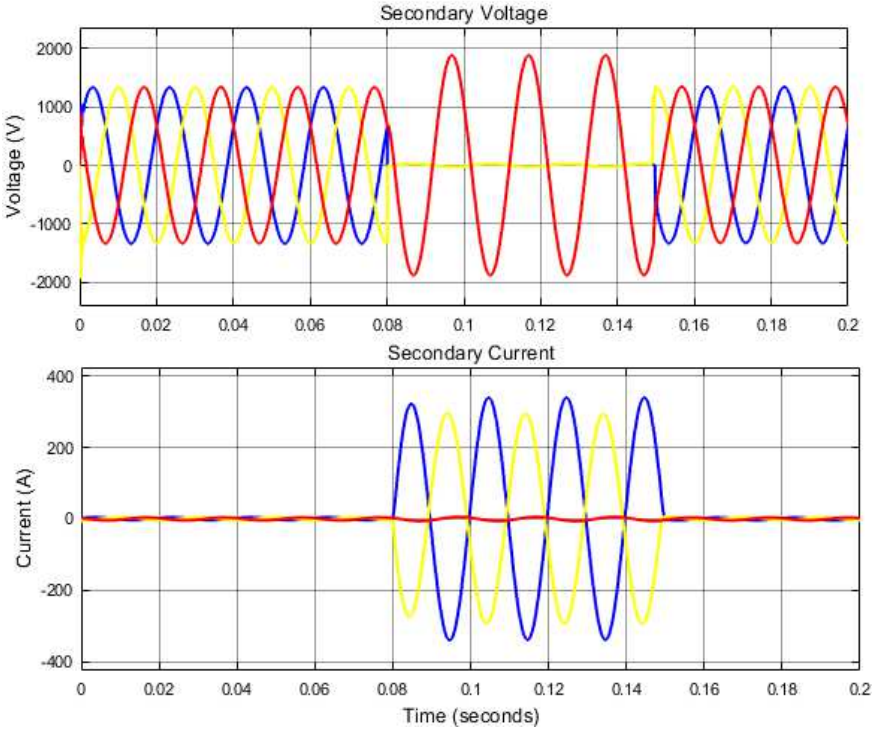

Figure 14. *Supply Voltage and Current under Line-Line-Ground Fault.*

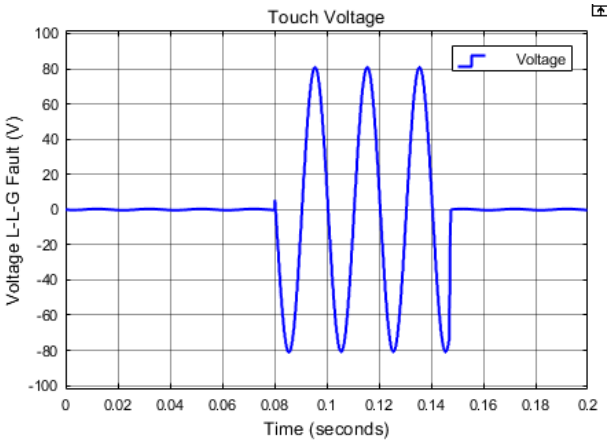

Figure 15. *Touch Voltage under Line-Line-Ground Fault.*

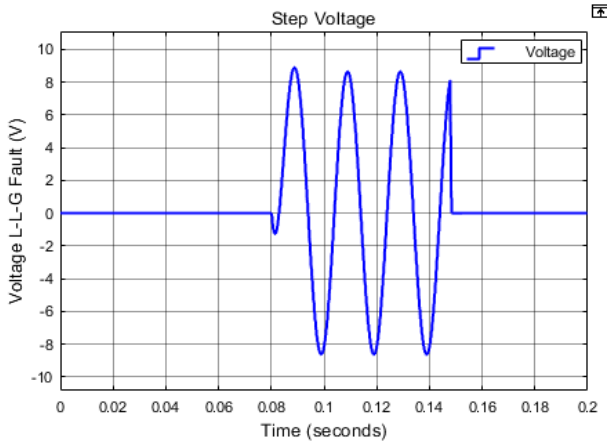

Figure 16. *Step Voltage under Line-Line-Ground Fault.*

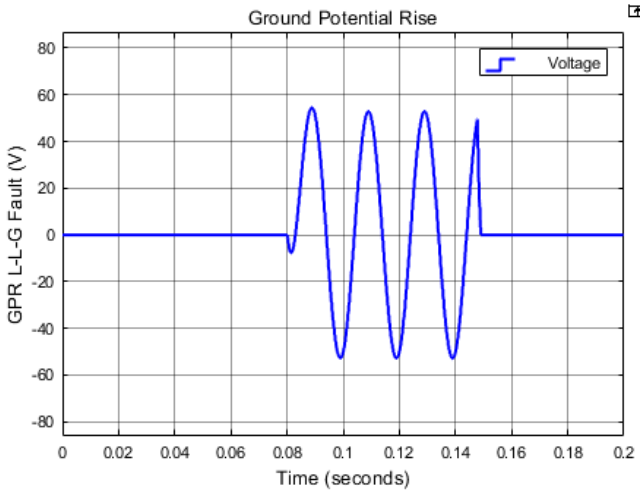

Figure 17. *Ground Potential Rise under Line-Line-Ground Fault.*

Concerning the impact of Line-Line-Ground faults on the system current, V. M. N. Dladla et al. [3] further suggest that the current magnitude of the affected phases that contact the ground rises significantly. This finding is observed in Figure 14 of the power system secondary current waveform when the fault is injected into the system between 0.08 and 0.15 seconds, the current magnitude of the faulted yellow and blue phase increases significantly. In Figure 14, the secondary voltage and current waveforms under the Line-Ground fault are shown, in Figures 15 to 17, the impact of the Line-Ground fault current on touch voltage, step voltage, and ground potential rise, are shown respectively.

5. Conclusion

In this paper, a 20 MVA, 88/22kV substation earth mat was designed, modeled, and simulated in ETAP and MATLAB/Simulink environment. The simulations and analyses conducted in ETAP included the assessment of different earth grid surface materials, and the different depths at which the surface materials are buried, this was conducted using crushed rocks. Further analyses were conducted in MATLAB/Simulink to assess the impact of asymmetrical faults (Line to Ground and Double Line to Ground) on the earth grid safety limits of touch voltage, step voltage, and ground potential rise.

From the analysis of the surface materials in ETAP, it was observed that the crusher run granite is the most effective surface material for earth grids as they have the smallest material resistivity and tolerable touch and step voltage limits compared to the other surface materials studied. Furthermore, the impact of the surface material depth was studied using the crushed rocks, and results show that the deeper the crushed rocks are buried into the ground, the higher the touch and step voltage tolerable limits get.

Analyses were conducted in MATLAB/Simulink to assess the impact of asymmetrical faults (Line to Ground and Double Line to Ground) on the safety limits of touch voltage, step voltage, and ground potential rise. From the simulations, it was observed that the type of fault on the substation determines the magnitude of touch voltage, step voltage, and ground potential rise, and this thread has an impact on the substation earth grid performance.

From the analyses conducted in this study, it is concluded that the crusher run granite stones are the most effective surface material and should be used for earth grid designs, also, the surface material should be buried as close to the surface as possible. Lastly, it is concluded that the type of system fault determines the magnitude of touch voltage, step voltage, and ground potential rise.

References

[1] B. Z. Nongena, A. F. Nnachi, R. P. Tshubwana, and C. G. Richards, "Substation Earth Grid modeling and simulation for Transient Performance Analysis," IEEE 62nd International Midwest Symposium on Circuits and Systems (MWSCAS), 2019, pp. 517-520.

[2] V. M. N. Dladla, A. F. Nnachi and R. P. Tshubwana, "Analysis of Varying Soil Resistivity on Substation Earthing Design and Performance Using ETAP," *2022 30th Southern African Universities Power Engineering Conference (SAUPEC)*, 2022, pp. 1-6.

[3] V. M. N. Dladla, A. F. Nnachi and R. P. Tshubwana, "The Impact of Different Fault Types on Touch Voltage, Step Voltage, and Ground Potential Rise," *2022 30th Southern African Universities Power Engineering Conference (SAUPEC)*, 2022, pp. 1-6.

[4] N. Jose, "Design of Earth Grid for a 33/11kV GIS Substation at a High Soil Resistivity Site using CYMGRD Software", International Journal of Engineering Research & Technology (IJERT), Vol 3 (10) October 2014, pp. 1151-1155.

[5] D. B. Desai, "Design and analysis of ground grid system for substation using E-TAP software and FDM code in MATLAB," International Journal of Engineering Research & Technology (IJERT), Vol. 7 (10), October 2018, pp. 51-53.

[6] D. Jacob, and K. Nithiyananthan, "Effective methods for lower systems grounding". WSEAS Transactions on business and economics. Vol. 5 (5) May 2008, pp. 151-160.

[7] V. P. Androvitsaneas, K. D. Damianaki, C. A. Christodoulou, and I. F. Gonos, I. F. "Effect of Soil Resistivity Measurement on the Safe Design of Grounding Systems". Energies 2020, 13, 3170. 2020.

[8] N. Permal, M. Osman, A. M. Ariffin, A. B. Abidin and M. Z. Kadir, "Effect of Non-Homogeneous Soil Characteristics on Substation Grounding-Grid Performances: A Review". Appl. Sci. 2021, 11, 7468, 2020.

[9] IEEE. "IEEE Std 80-2013: IEEE Guide for Safety in AC Substation Grounding," The Institute of Electrical and Electronics Engineers, Inc. New York, January 2000A. Salam and Q. M. Rahman, "'Soil Resistivity', in Power Systems Grounding," Singapore: Springer Science + Business Media Singapore. 2016.

[10] IEEE, "IEEE Std 81-2012: IEEE Guide for Measuring Earth Resistivity, Ground Impedance, and Earth Surface Potentials of a Grounding System". The Institute of Electrical and Electronics Engineers, Inc. New York, December 2012.

[11] L. L, Win, K. T, Soe, "Design Consideration of Electrical Earthing System for High-rise Building," American Scientific Research Journal for Engineering, Technology, and Sciences (ASRJETS). Vol 26 (2) 2016, pp. 270-282.

[12] H. N. Amadi, "Soil Resistivity Investigations for Substation Grounding Systems In Wetland Regions – A Case Study Of Lagos State, Nigeria," Asian Journal of Natural & Applied Sciences. Vol 6 (4), December 2017, pp. 94-95.

[13] O. E. Gouda O. E, G. M. Amer and T. M. El-Saied, "Factors affecting the apparent soil resistivity of multi-layer Soil," Proceedings of 14th International Symposium on High Voltage Engineering (ISH 2005), Beijing, China, August 25-29, 2005.

[14] A. Salam and Q. M. Rahman, "'Soil Resistivity', in Power Systems Grounding," Singapore: Springer Science + Business Media Singapore. 2016.

[15] A. Patil, "Substation Earthing Design," IOSR Journal of Electrical and Electronics Engineering (IOSR-JEEE), Vol. 12 (1) Ver. II, January 2017, pp. 12-17.

[16] D. Sweeting, "Applying IEC 60909, Fault Current Calculations," IEEE Trans. Industry App., vol. 48, no. 2, March/April 2012., pp. 575-580.

[17] K. S. Ratnadeep, Y. N. Bhosale, S. Kulkarni, "Fault Level Analysis of Power Distribution System," 2013 International Conference on Energy Efficient Technologies for Sustainability – Nagercoil. April 2013.

[18] A. Salam and Q. M. Rahman, "'Ground Resistance Measurement', in Power Systems Grounding," Singapore: Springer Science + Business Media Singapore. 2016.

[19] Fluke Corporation, “Earth Grounding Resistance – Principles, Testing Methods and Applications,” Everett: Fluke Corporation, 2013, pp 3-5.

[20] V. M. N. Dladla, A. F. Nnachi and R. P. Tshubwana, "The Impact of System Fault Level on the Design of a Substation Earthing Grid Simulation Using ETAP," *2022 30th Southern African Universities Power Engineering Conference (SAUPEC)*, 2022, pp. 1-6.

[21] A. G. Swanson, M. Brown, K. Moodley and A. Singh, "Resistivity of Surface Materials for Substation Earthing," 2020 IEEE PES/IAS Power Africa, 2020, pp. 1-5.